

Mechanical Properties of Haynes® Alloy 188 after Exposure to LiF-22CaF_2, Air, and Vacuum at 1093 K for Periods up to 10,000 Hours

J.D. Whittenberger

As part of a program to provide reassurance that the cobalt-base superalloy Haynes® Alloy 188 can adequately contain a LiF-CaF_2 eutectic thermal energy storage salt, 4900- and 10,000-hr exposures of Haynes® Alloy 188 to LiF-22CaF_2, its vapor, vacuum, and air at 1093 K have been undertaken. Following such exposures, the microstructure has been characterized and the 77 to 1200 K tensile properties measured. In addition, 1050 K vacuum creep-rupture testing of as-received and molten salt- and vacuum-exposed samples has been undertaken. Although slight degradation of the mechanical properties of Haynes® Alloy 188 due to prior exposure was observed, basically none of the losses could be ascribed to a particular environment. Hence, observed decreases in properties are due to thermal aging effects, not corrosive attack. In view of these findings, Haynes® Alloy 188 is still deemed to be suitable for containment of the eutectic LiF-CaF_2 thermal energy storage media.

1. Introduction

ONE concept to provide Space Station Freedom with a continuous supply of heat and electrical power involved the use of a solar dynamic system.[1] In this case, a focused mirror guides and concentrates solar energy into a heat receiver. By circulating an inert gas through the receiver, heat can be directed to a Brayton engine that powers an electrical generator and/or sent to a thermal energy storage unit. Although material problems exist for all solar dynamic components, the suggested use of the latent heat of fusion of fluoride salt eutectics to store energy leads to specific concerns, because molten fluorides tend to be very corrosive.

The initial design of the space-based solar dynamic system was established with a relatively low-temperature Brayton Cycle heat engine operating at ~1015 K to allow usage of the conventional cobalt-base superalloy Haynes® Alloy 188 (referred to as alloy 188) for the high-temperature hardware and the LiF-20CaF_2* eutectic that melts at 1043 K for the energy storage medium.[2] Alloy 188 was chosen as the salt containment alloy as a result of previous compatibility experiments with LiF-superalloy combinations and its excellent long-term 1000 to 1200 K creep-rupture strength in combination with ease of fabricability and weldability. LiF-20CaF_2 was selected on the basis of its high heat of fusion in combination with a relatively low melting point, which would limit the degree of chromium sublimation from the vacuum-exposed containment alloy.

Concurrent with the choice of energy storage salt and containment alloy, compatibility studies were started at Boeing,[3] AiResearch,[4,5] and the Lewis Research Center[2] to provide reassurance that alloy 188 would be able to withstand the corrosive attack of the LiF-CaF_2 eutectic. Cotton and Sedgwick[3] found only very slight intergranular attack of alloy 188 after 100, 500, 2000, or 5000 hr of exposure to molten salt at 1144 K. Strumpf *et al.*[4,5] cycled eutectic salt-filled alloy 188 capsules in air to simulate melting/freezing conditions (600 sec ramp from 810 to 1115 K, 1800 sec hold at temperature, fast cool down over 600 sec from 1115 to 1000 K, followed by slower cooling to 810 K in 3300 sec) for various periods up to 20,013 hr. They also found only very minor intergranular pitting that was attributed to entrained contaminants, because the degree of the attack was essentially independent of exposure time. Strumpf *et al.*[4,5] additionally reported the development of thin chromium-depleted (~30 μm) regions and chromium-rich films (~2 μm) inside some of the capsules. These areas were thought to be the result of thermal gradients induced within the capsules during the temperature cycles. In essence, chromium was being volatilized from the hot regions and deposited at the cold regions. Because such a phenomenon would be diffusion controlled, it was concluded[5] that no significant chromium depletion of the alloy would occur over the proposed 30-year lifetime of the solar dynamic system.

To investigate the effect of salt exposure on the mechanical properties of alloy 188 beyond that attributed to simple thermal exposure, Strumpf *et al.*[4,5] machined miniature specimens from the exposed capsules and tensile tested these at room temperature. Their results are reproduced in Fig. 1, in which it can be seen that prior exposure had only a slight effect on 0.2% yield and ultimate tensile strengths, but significantly reduced the residual ductility. Such a loss in elongation was expected, because Haynes International data[6] indicate that the 50% ductility for as-received material is reduced to 9% after an 8000-hr heat treatment in air at 1033 K. In terms of the long life proposed for the solar dynamic system, the mechanical-property data in Fig. 1 are most encouraging. However, it should be noted that these experiments were not scientifically "clean." In particular, the mechanical-property specimens were cut from material that was exposed to two different environmental conditions—LiF-20CaF_2 on one side and air on the other side. In

J.D. Whittenberger, NASA Lewis Research Center, Cleveland, Ohio.

*All compositions in mole percent unless noted.

addition, the 20,013 hr of cyclic exposure only translates to slightly over 5700 hr at the maximum temperature.

To provide confidence that mechanical behavior is not unexpectedly affected, NASA has instituted a program to (1) expose superalloys to the molten LiF-CaF_2 eutectic, its vapor, and vacuum at 1093 K for periods up to 2.25×10^4 hr and (2) measure the post-exposure tensile properties from 77 to 1200 K and the post-exposure creep-rupture characteristics at 1050 K. An initial paper[2] reported the preliminary results in terms of weight change, microstructure, and tensile properties for alloy 188 and the nickel-base alloy Haynes Alloy® 230 exposed to LiF-22CaF_2, the nominal eutectic composition, and vacuum for 400 and 2500 hr. This article concentrates on the behavior of alloy 188 after being exposed for longer periods, up to 10^4 hr, to salt and vacuum. In addition, the effects of long-term exposure to air at 1093 K were also examined to provide a comparison between the behavior in nontraditional environments and a common terrestrial condition.

2. Experimental Procedures

Full details describing the tensile specimen fabrication, methodology of salt and vacuum exposures, and the mechanical-property testing have been previously reported.[2] The following provides a general characterization of the experimental procedures, except where they differ from those described in Ref. 2 or where additional work was involved.

To obtain a statistically meaningful measure of degradation due to long-term exposure, it was felt that a large number of mechanical-property tests of exposed samples must be undertaken. Therefore, closed "bread pan" capsules[2,7,8] were assembled, which contained two racks of tensile specimens (~50 samples/rack). At temperature, the lower rack was immersed in the liquid LiF-CaF_2 eutectic while the second rested on tabs and was exposed to the salt vapor. After vacuum sealing each capsule, a third rack was placed on top, and the whole assembly was introduced into a vacuum furnace for heat treatment.

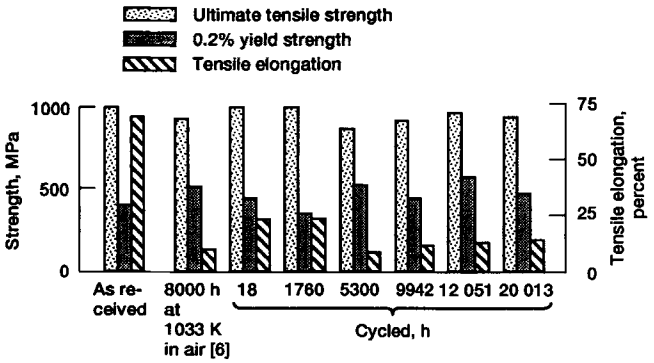

Fig. 1 Room-temperature tensile properties of as-received alloy 188 specimens and of alloy samples annealed for 8000 hr at 1033 K in air[6] or machined from LiF-19.5CaF_2-filled thermal energy storage capsules that were subjected to long-term cyclic exposures in air from 810 to 1115 K.[4,5]

Approximately 1.27-mm-thick by 0.6-m by 1.2-m sheets of alloy 188 (Table 1) were purchased from Haynes International for this study. From this stock, bread pan capsules, about 280 mm long by 140 mm high and 115 mm wide, with matching lids were fabricated by a combination of bending and welding without using foreign metal as filler. For simplicity and ease of fabrication, pin and clevis tensile-type specimens (108 mm long by 19 mm wide with a 31.8-mm by 9.8-mm gage section) were directly punched from the alloy sheet, with the gage length parallel to the sheet rolling direction. All bread pan components and tensile specimens were cut from the same heat of alloy 188 sheet, which was supplied in a solution-treated condition with silver metallic sheen. Polished and etched metallurgical sections revealed that this alloy had a reasonably uniform, equiaxed grain structure, with an average diameter of ~20 μm, as shown in Fig. 2(a).

The tensile specimens were cleaned, weighed, measured, and then placed in specimen racks. With a rack of specimens on the bottom of the capsule, about 2.6 kg of 1-mm or smaller diameter LiF-22CaF_2 chunks (Table 1) were poured into the bread pan. After placing the second rack on the tabs within the capsule, the lid, which contained two ~3-mm holes, was tungsten inert gas (TIG) welded to the main body in an argon atmosphere. This assembly was then slowly heated to 1093 K under vacuum (4 hr from room temperature to 993 K, 2 hr to 1093 K, followed by 1 hr hold at temperature, and a furnace cool) to remove dissolved gases and water from the salt. Directly after this heat treatment, the vents were closed by electron beam welding.

Bread pan capsules with a third rack of specimens on top were exposed for 4900 and 10,000 hr at 1093 K in a cryogenically pumped vacuum of $\sim 1.3 \times 10^{-4}$ Pa or less. None of these exposures were continuous; shut downs due to loss of electrical power or cooling water, vacuum leaks, regeneration of the cryopumps (approximately every 400 hr), *etc.*, were experienced. Upon completion of the planned corrosion experiment, the capsules were cut open, photographed, and several samples of frozen salt were taken for chemical analysis. Prior to measuring and weighing, the molten salt-exposed specimens were wiped with a clean, lint-free cloth. The vacuum-annealed samples were not cleaned prior to post-exposure measurements.

Racks of approximately 50 tensile specimens were also exposed in air at 1093 K for 4900 and 10,000 hr. As was the case for the vacuum exposure, none of these heat treatments were continuous; however, the number of disruptions were far fewer than those experienced by samples within the vacuum furnaces.

Table 1 Characterization of Starting Materials

Material	Vendor	Heat/lot	Composition, wt.%
Haynes® Alloy 188.....	Cabot Corp.	188061773	0.005 B, 0.11 C, 21.69 Cr, 1.95 Fe, 0.048 La, 0.72 Mn, 23.03 Ni, 0.013 P, <0.002 S, 0.38 Si, 14.02 W, Co
Salt	Cerac Inc.	23590-A-5-12	<0.001 Al, <0.001 Cu, 0.005 Fe, 14.6 Li, 0.005 Mg, 0.001 Si; LiF – 21.7 mol% CaF_2

The air-exposed specimens were handled in the same manner as the vacuum-exposed tensile specimens; in particular, they were not cleaned prior to post-exposure weighing.

Triplicate tensile tests at 77, 298, 750, 900, 1050, and 1200 K were conducted under contracts at the Surface Engineering Center of the IIT Research Institute (NAS3-24976) and the

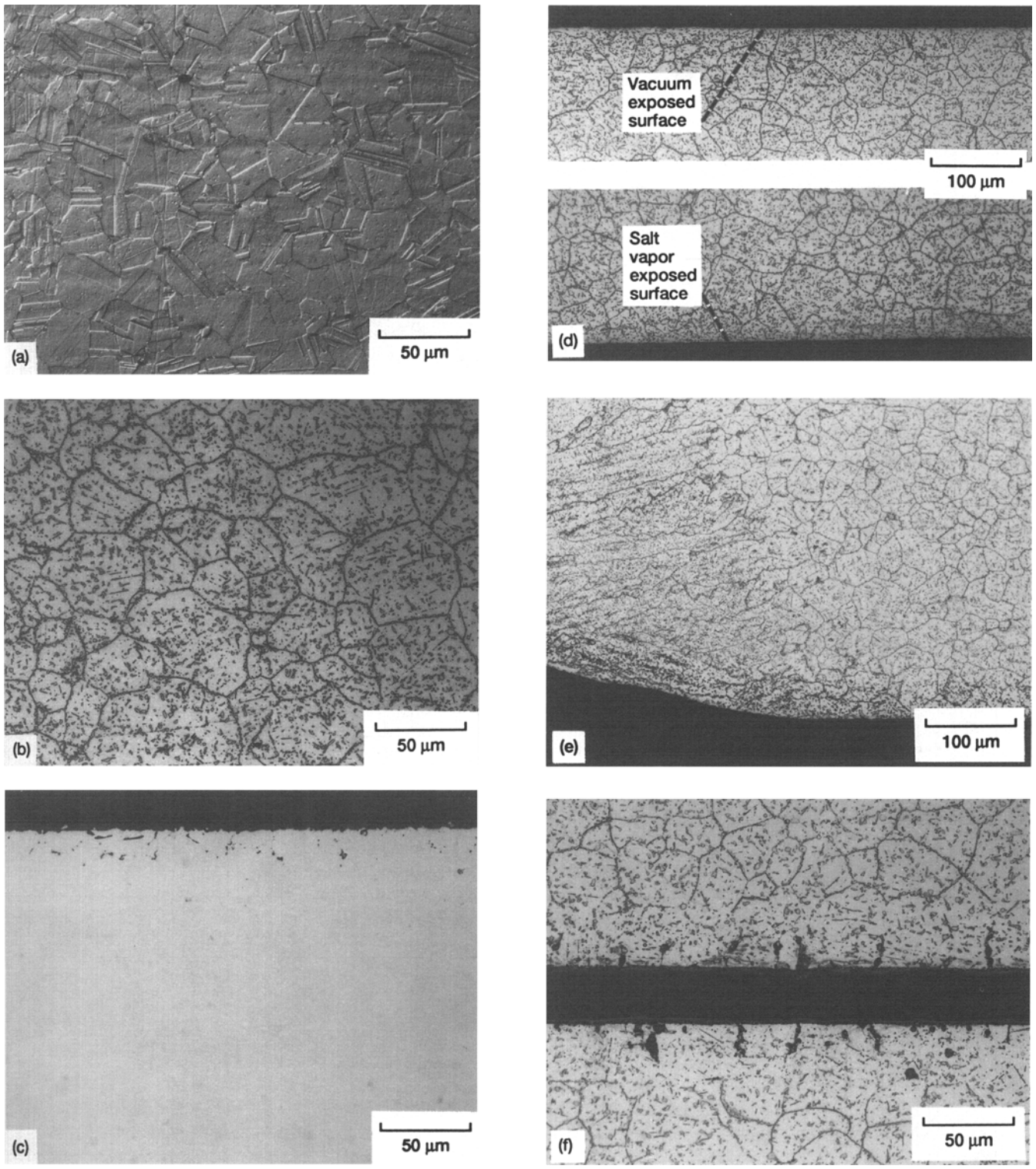

Fig. 2 Typical microstructures found in as-received Haynes® Alloy 188 (**a**) and in alloy specimens exposed at 1093 K (**b-f**). (**b**) Annealed for 10,000 hr. (**c**) Molten LiF-22CaF_2-exposed surface after 4900 hr. (**d**) Salt vapor- and vacuum-exposed surfaces after 10,000 hr. (**e**) TIG weld exposed to vacuum for 10,000 hr. (**f**) Air-exposed surface after 10,000 hr. All parts except (**c**) have been etched.

Cortest Laboratories, Inc. (NAS3-25759) on LiF-CaF_2 eutectic salt-exposed, vacuum-annealed air-exposed, and as-received specimens. All 77 K tensile tests were conducted in liquid N_2, whereas the 298 K tests were undertaken in air. For testing at and above 750 K, the salt/vacuum-exposed samples were tested in vacuum ($<10^{-3}$ Pa), whereas the air-exposed samples were tested in air. Typical test data included 0.02 and 0.2% offset yield strengths, ultimate tensile strength (UTS), and elongation at failure; all mechanical properties were calculated on the basis of the original (pre-exposure) dimensions.

1050 K vacuum ($<10^{-3}$ Pa) creep-rupture testing was also accomplished under contracts NAS3-24976 and NAS3-25759 where testing was limited to samples exposed either in vacuum or liquid LiF-22CaF_2. A typical series for each exposure condition consisted of eight samples tested at engineering stress levels designed to produce failure in 10 to 1500 hr. Data to be gathered included time to 0.1, 0.2, 0.5, 1, 2, 5, and 10% strain, steady-state creep rate, and failure time and elongation.

Standard metallographic procedures, X-ray methods, and chemical analysis were utilized to characterize the starting, exposed, and tensile-tested materials. Polished metallographic sections of as-received alloy 188 were immersion etched with a mixture of 80 ml^3 HCl and 8 ml^3 H_2O_2, whereas exposed material was electrolytically etched at 4 V and 0.5 A in 95 ml^3 H_2O plus 5 ml^3 HCl or 95 ml^3 H_2O plus 5 ml^3 HF.

3. Results

3.1 *Exposures*

3.1.1 *Salt/Vacuum*

LiF-22CaF_2-filled alloy 188 capsules were successfully vacuum heat treated for 4900 and 10,000 hr at 1093 K without major difficulty. It should be noted, however, that the 4900-hr capsule did develop a small leak in the lid/main body weld during the heat treatment, which allowed some of the higher vapor pressure LiF to escape. This leak was found during the first inspection after ~910 hr of exposure. This defect probably originated in the original welding pass. No such faults were found in the 10,000-hr capsule. The exterior (vacuum-exposed) surface of both alloy 188 capsules and their respective vacuum-exposed specimens were basically unblemished and possessed a silvery metallic sheen.

A photograph of an opened alloy 188 bread pan after heat treating at 1093 K in a vacuum furnace is presented in Fig. 3. Both the 4900- and 10,000-hr capsules were identical in appearance, where the lower rack of specimens was completely immersed in frozen salt while the upper rack was maintained above the molten LiF-22CaF_2 in the salt vapor. The inner surfaces of the bread pans and the alloy 188 specimens exposed to LiF-22CaF_2 vapor were bright metallic without any visible sign of corrosion (Fig. 3). In both cases, some vapor-exposed specimens had small droplets of frozen salt on the surface. Before weighing, as many as possible of these salt drops were removed by scratching with a gloved hand.

The frozen blocks of LiF-22CaF_2 did not adhere to the capsule walls, and in general, the salt was dull gray in appearance; however, chemical analysis of several samples from each capsule failed to reveal any instance of contamination by likely elements (Co, Cr, Fe, *etc.*, Table 1). Additionally, materialographic examination of the frozen salt taken from each capsule confirmed that the LiF-22CaF_2 possessed a typical lamellar eutectic microstructure.

The tensile specimens encapsulated in the solidified salt were broken free by judicious use of a hammer and mechanical manipulation. Once freed, the molten exposed alloy 188 specimens were found to have a mottled gray, metallic appearance. Although the solidified LiF-22CaF_2 did not adhere to the 4900-hr specimens, minor salt deposits were tenaciously bonded to several alloy 188 samples exposed for 10,000 hr. This material was removed, as completely as practical, by scratching with metal spatula prior to weighing.

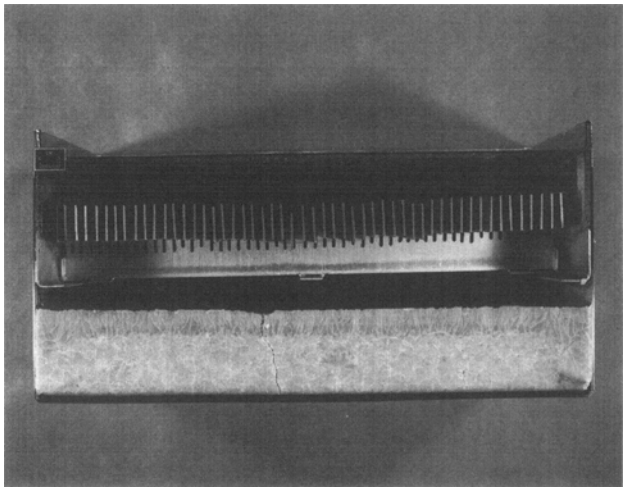

Fig. 3 Opened Haynes® Alloy 188 bread pan capsule after heat treatment in vacuum at 1093 K for 10,000 hr.

Table 2 Statistical Summary of Weight Changes Found in As-Received Haynes® Alloy 188 Tensile-Type Specimens after Exposure to Molten LiF-22CaF_2, Salt Vapor, or Vacuum at 1093 K

	Weight change, mg, after exposure to:		
	Molten salt	Salt vapor	Vacuum
After 4900 hr of exposure			
Average	–6.5	2.2	–5.7
Standard deviation	1.1	0.5	1.4
Maximum	–3.5	3.5	–4.0
Minimum	–8.2	0.9	–11.6
After 10,000 hr of exposure			
Average	–4.8	4.2	–9.1
Standard deviation	1.8	1.7	2.1
Maximum	0.0	7.1	–7.3
Minimum	–7.4	–0.5	–19.2

Note: The data represent results from at least 50 tensile-type specimens where each sample was ~1.3 mm thick, weighed about 17 g, and had approximately 33 cm^2 of surface area.

A statistical summary of the weight change results for each exposure condition is outlined in Table 2. These data indicate that the samples immersed in molten LiF-22CaF_2 or exposed to vacuum underwent some weight loss, whereas the vapor-exposed samples gained a slight amount of weight. Comparison of the 4900-hr exposure data to that after 10,000 hr shows about the same average weight loss after immersion in molten salt; likewise, the average weight gain is about the same for salt vapor-exposed samples. However, the average weight loss after vacuum exposure is about 60% greater for the longer exposure time (–9.1 mg versus –5.7 mg). Based on the original weight and surface area of each specimen, such changes are small, and for all practical purposes, they are negligible (<2 mg/cm^2) even in the worst case. Thus, the results indicate that the salt does not grossly attack alloy 188, whereas exposure to vacuum produces continuous loss of volatile alloying specimens (chromium and manganese).

Metallurgical specimens taken from both the vacuum heat treated bread pans revealed that long-term annealing led to precipitation of M_6C carbides,[2] which both decorated grain boundaries and occurred intragranularly (Fig. 2b). Grain size measurements on the heat treated alloys indicated that the average diameter was ~27 μm after 4900 hr of exposure and ~30 μm after 10,000 hr, where the standard deviation for both of these estimates is ~5 μm. Because these values are larger than the as-received grain size (~20 μm), it appears that some grain growth has taken place.

Examination of the alloy 188 surface in contact with the molten salt revealed signs of degradation, as grain boundary pits and irregular surfaces were observed (Fig. 2c). However, measurement of the depth of pitting revealed that it was not dependent on the time of exposure, with the average penetration (as measured on unetched samples) being ~17 μm (standard deviation of about 3 μm) after either 4900 or 10,000 hr at temperature. No evidence of surface attack was visible in alloy 188 subject to long-term exposure to either salt vapor or vacuum (Fig. 2d), nor was any sign of corrosion found at the liquid/vapor salt interfaces. Lastly, examination of the tungsten inert gas welds exposed to either salt or vacuum did not reveal any unusual behavior either in the weld itself or in the heat-affected zones (Fig. 2e).

Table 3 Statistical Summary of Weight Changes Found in As-Received Haynes® Alloy 188 Tensile-Type Specimens after Exposure to Air at 1093 K

	Weight change, mg, after exposure for: 4900 hr	10,000 hr
Average	15.1	28.6
Standard deviation	3.1	2.8
Maximum	20.3	33.5
Minimum	8.7	21.6

Note: The data represent results from at least 50 tensile-type specimens where each sample was ~1.3 mm thick, weighed about 17 g, and had approximately 33 cm^2 of surface area.

3.1.2 *Air*

After 4900 or 10,000 hr of exposure to air at 1093 K, the tensile samples were covered with a dark brown-black oxide scale, which was identified by X-ray diffraction techniques to consist of a spinel (probably $CoCr_2O_4$) in combination with Cr_2O_3. Table 3 summarizes the weight change data, which clearly show that heat treatment in air leads to weight gain via oxidation. These data also indicate that doubling the time of exposure leads to about twice the weight gain. For either condition, however, the change on a mg/cm^2 basis is quite small, *e.g.*, <1 mg/cm^2.

Although no differences in grain size or carbide precipitation were found between the air and salt/vacuum-exposed alloy, prolonged heat treatment in air did result in grain boundary

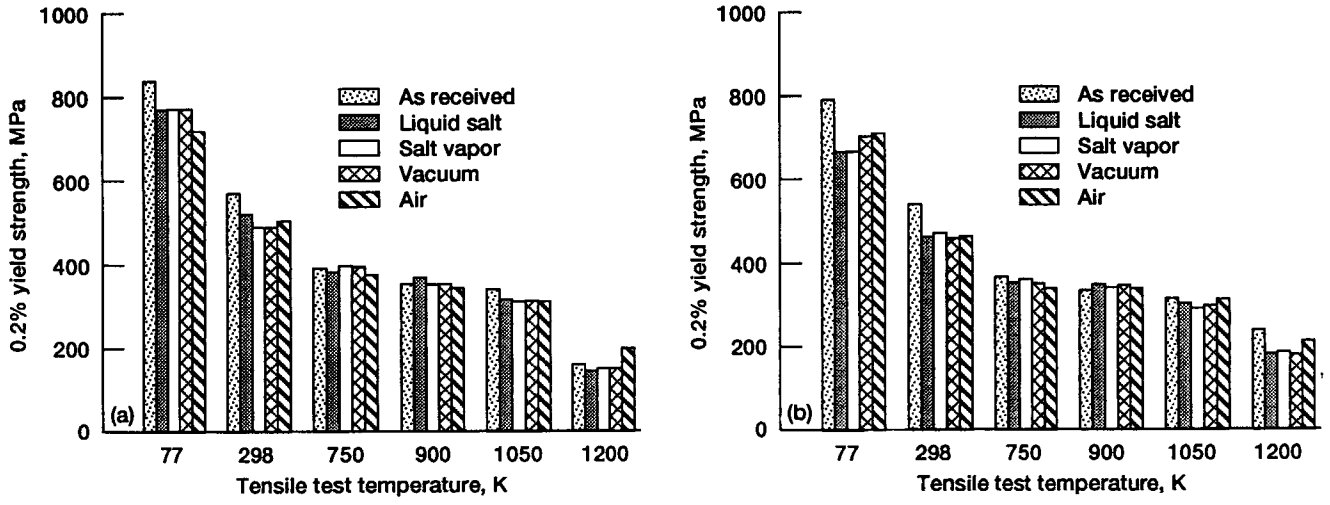

Fig. 4 Average 0.2% yield strength of Haynes® Alloy as a function of testing temperature and prior 1093 K exposure for 4900 hr (**a**) and 10,000 hr (**b**) in various environments.

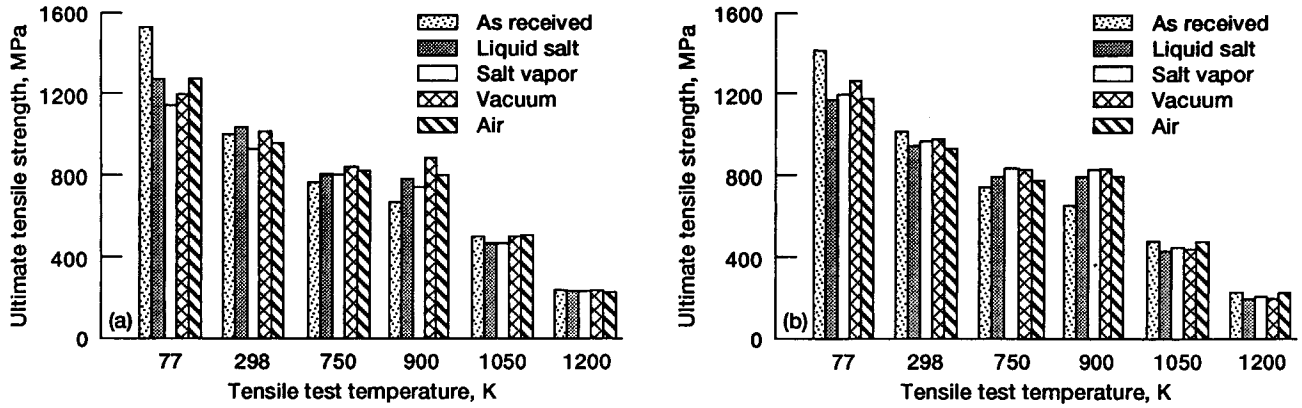

Fig. 5 Average ultimate tensile strength of Haynes® Alloy as a function of testing temperature and prior 1093 K exposure for 4900 hr (**a**) and 10,000 hr (**b**) in various environments.

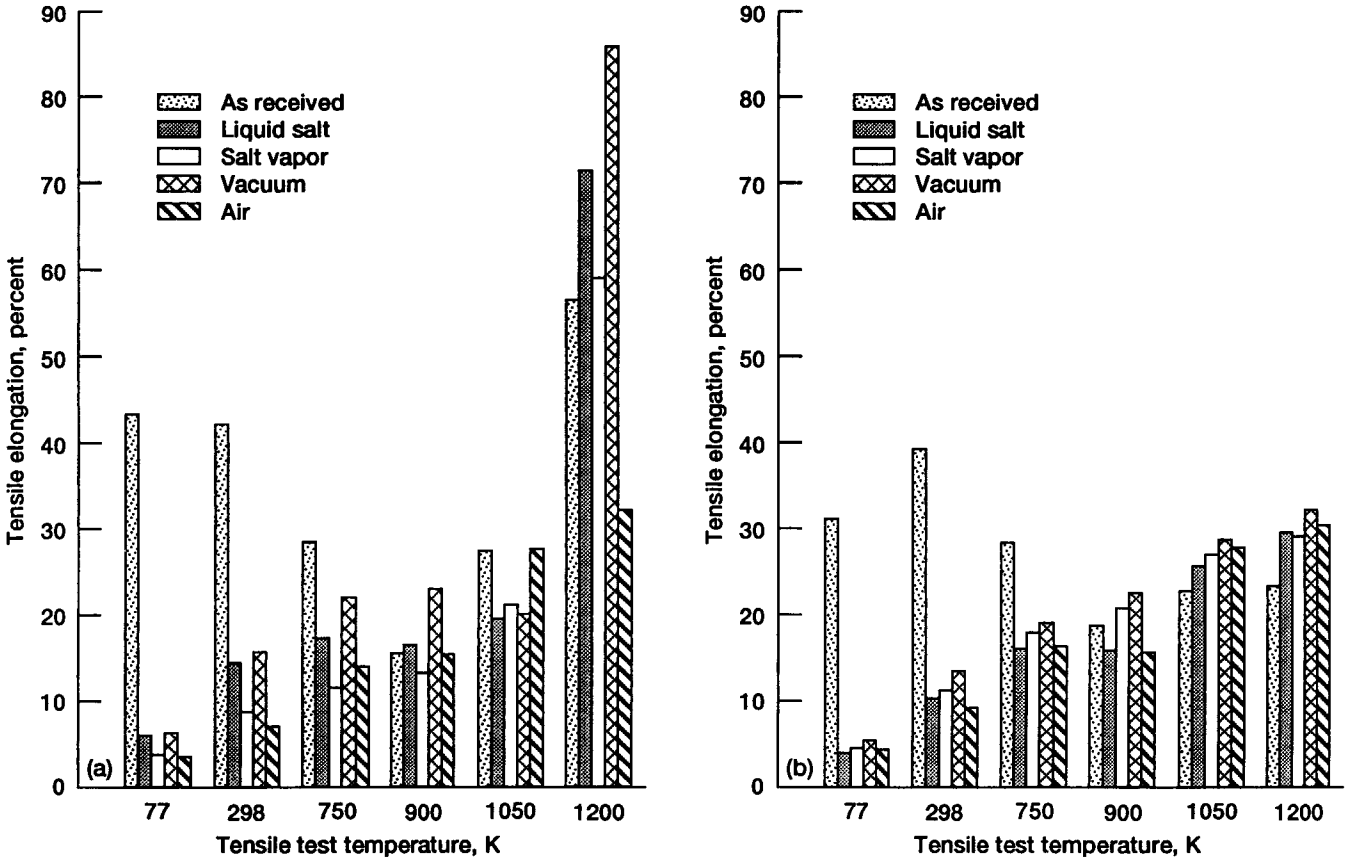

Fig. 6 Average tensile elongation of Haynes® Alloy as a function of testing temperature and prior 1093 K exposure for 4900 hr (**a**) and 10,000 hr (**b**) in various environments.

pits, as evidenced by the near-surface porosity in Fig. 2(f). Measurement of the depth of the pitting indicated that the degree of attack increased with time, where the average penetration measured on unetched samples was ~10 μm after 4900 hr of exposure and about 20 μm after 10,000 hr, with both values having a standard deviation of ~4 μm.

3.2 *Tensile Testing*

Bar diagrams illustrating the effects of the various environments and time of exposure on the average 0.2% yield strength, ultimate tensile strength, and tensile elongation are presented in Fig. 4 through 6, respectively, and statistical summaries (av-

Table 4 Tensile Properties of Haynes® Alloy after Various 4900-hr Exposures at 1093 K

0.02% yield stress, MPa		0.2% yield stress, MPa		UTS, MPa		Elongation, %	
Average	Standard deviation	Average	Standard deviation	Average	Standard deviation	Average	Standard deviation
As received, tested in vacuum							
759.0	66.5	844.0	37.6	1527.7	6.6	43.3	2.4
531.7	102.6	573.0	85.2	1002.3	25.8	42.3	4.8
373.7	10.2	395.3	6.2	767.3	13.7	28.3	0.9
332.3	11.5	357.3	8.8	671.7	15.5	15.3	5.2
317.7	11.0	345.7	5.2	507.7	4.8	27.3	1.7
141.0	10.8	163.7	11.3	243.3	4.2	56.0	27.0
Molten LiF-22CaF$_2$, tested in vacuum							
688.7	27.5	776.7	16.5	1266.7	119.2	5.7	0.5
460.7	13.1	522.3	6.6	1035.0	62.8	14.3	2.1
335.3	18.4	389.3	9.0	806.0	33.3	17.3	4.0
334.3	6.6	373.7	7.4	785.7	59.7	16.0	3.6
287.3	7.8	320.7	7.8	479.0	9.9	19.0	1.6
126.0	4.5	144.7	4.0	240.3	16.0	71.0	11.9
LiF-22CaF$_2$ vapor, tested in vacuum							
690.0	11.5	779.0	4.3	1135.7	25.7	3.7	0.5
433.7	18.9	491.7	23.5	925.0	37.5	8.7	1.2
353.0	8.0	399.7	9.7	803.3	19.1	11.3	1.2
317.3	2.6	356.3	1.7	748.0	11.0	13.0	1.6
286.0	6.5	318.0	7.1	474.7	9.5	20.7	1.2
126.0	12.0	152.7	12.3	238.0	21.2	58.7	12.5
Vacuum, tested in vacuum							
660.0	38.8	748.0	32.8	1199.7	5.6	6.0	0.0
411.0	13.1	490.3	18.8	1012.3	31.7	15.7	2.1
316.3	42.5	381.0	14.2	844.3	20.1	22.0	3.7
350.7	21.7	385.7	21.8	887.7	37.9	22.7	0.9
289.0	4.3	320.3	1.2	505.7	8.7	19.7	1.7
134.3	10.1	154.7	14.1	243.7	20.8	86.0	6.5
Air exposure, tested in air							
607.7	91.4	725.6	72.2	1272.5	61.1	3.4	0.5
408.2	60.7	506.4	27.0	956.6	50.9	6.9	1.0
336.0	12.5	380.5	6.4	822.3	28.0	13.7	2.2
318.8	10.5	348.5	8.7	805.8	27.7	15.1	0.3
278.4	13.9	318.0	21.2	510.4	8.4	27.3	1.5
180.6	3.3	202.1	3.2	233.2	4.7	32.0	0.8

erage value and standard deviation) of the tensile test results, including the 0.02% yield strengths, are given in Tables 4 and 5. Because the elevated temperature (≥750 K) properties for the as-received alloy were measured in both vacuum and air, part (a) of Fig. 4 through 6 (and Table 4) presents results from the vacuum testing of the as-received alloy 188, whereas part (b) of these figures (and Table 5) reports the data from air testing of as-received alloy. Lastly, it should be noted that the elevated temperature tensile tests conducted on the 10,000-hr salt/vacuum-exposed specimens were inadvertently conducted in air instead of vacuum.

3.2.1 *Yield Strength*

Testing of as-received alloy 188 in either air or vacuum produced 0.2% yield stress values (Fig. 4) that were within 10% at each temperature except at 1200 K, where air testing yielded an approximately 70 MPa higher advantage (Fig. 4b). In general, prior exposure to either salt, vacuum, or air somewhat reduced the yield strength; however, no one specific environment produced more degradation than the others. Furthermore, by comparison of Fig. 4(a) and (b), it appears that the degree of softening increases with increasing time of exposure. Although there are some specific differences (*i.e.*, the 1200 K tensile results after 4900 and 10,000 hr), the 0.02% yield strength (Tables 4 and 5) follows the same trends.

3.2.2 *Ultimate Tensile Strength*

Comparison of the ultimate tensile strength measured at each test temperature for the as-received alloy reveals little, if any, difference between those measured in vacuum (Fig. 5a) or air (Fig. 5b). Again, the data obtained for specimens exposed to various environments do not reveal any consistent pattern of behavior. All four prior exposures (molten LiF-22CaF$_2$, salt vapor, vacuum, or air at 1093 K) affected the ultimate tensile strengths in a like manner, where the 77 and 298 K and 1050 and 1200 K ultimate tensile strengths were reduced relative to the as-received values, and the 750 and 900 K values of the exposed samples were greater than the as-received properties. As opposed to the observed tendency for the 0.2% yield strength

Table 5 Tensile Properties of Haynes® Alloy after Various 10,000-hr Exposures at 1093 K

0.02% yield stress, MPa		0.2% yield stress, MPa		UTS, MPa		Elongation, %	
Average	Standard deviation	Average	Standard deviation	Average	Standard deviation	Average	Standard deviation
As received, tested in air							
677.5	25.1	790.4	25.8	1435.4	73.8	31.5	3.9
430.3	73.6	540.3	7.5	1027.1	7.2	39.8	1.2
331.2	5.9	362.5	1.5	755.0	3.4	28.6	0.8
313.8	2.5	335.4	5.9	667.8	3.7	19.1	0.7
286.7	5.3	309.6	3.7	489.3	12.5	23.1	5.3
210.5	6.3	234.2	8.4	235.6	9.1	23.7	3.5
Molten LiF-22CaF$_2$, tested in air							
449.9	52.6	666.3	64.5	1189.4	100.6	3.9	1.4
389.6	21.9	462.2	10.0	965.4	24.8	10.6	0.7
299.6	2.1	349.0	3.5	812.3	4.9	16.3	1.2
310.4	22.6	345.5	22.1	806.1	18.5	16.0	1.7
264.7	6.0	296.6	5.8	442.2	2.4	26.0	0.0
149.5	6.5	176.7	3.3	202.2	2.8	30.1	1.6
LiF-22CaF$_2$ vapor, tested in air							
582.5	77.7	666.2	73.4	1209.1	70.9	4.3	0.9
393.0	10.3	466.0	9.8	981.0	24.8	11.4	1.2
305.0	22.3	359.7	21.1	847.2	35.5	18.1	2.4
297.1	14.2	343.0	21.6	837.6	24.5	21.1	2.0
245.6	5.7	290.1	1.9	455.0	6.7	27.4	0.7
150.1	6.6	177.0	5.2	207.0	8.6	29.5	0.9
Vacuum, tested in air							
594.6	83.0	699.6	83.8	1281.1	73.1	5.3	1.2
387.7	15.2	457.4	10.2	993.7	24.0	13.4	0.8
285.4	13.3	347.6	7.1	840.3	8.6	19.3	0.4
306.4	12.3	343.6	8.4	844.9	3.1	23.0	0.6
249.1	9.1	293.5	7.8	449.3	6.9	29.1	0.1
150.9	6.9	173.1	7.5	201.9	4.3	32.6	0.3
Air exposure, tested in air							
579.2	19.2	708.6	35.9	1187.9	12.1	4.4	0.2
388.3	32.5	458.0	19.3	951.7	45.6	9.3	0.5
306.2	4.3	335.8	1.5	789.9	20.5	16.6	3.7
315.2	13.0	336.9	11.8	810.1	7.7	15.9	1.4
275.3	17.4	306.9	18.1	484.5	6.0	28.2	1.9
189.3	3.8	206.3	2.2	229.5	5.2	30.8	2.4

(Fig. 4), increased exposure time does not reduce the ultimate tensile strength for alloy 188 (Fig. 5).

3.2.3 *Tensile Elongation*

Although both air and vacuum testing of as-received alloy 188 (Fig. 6a and b) indicate that this alloy is ductile, with extensions exceeding 15% at all six test temperatures, the tensile elongations measured in vacuum at 77 and 1200 K (Fig. 6a) are greater than those determined in air at these two temperatures (Fig. 6b). It is thought[2] that these two discrepancies are most likely due to the specimen fabrication technique (punching in the present study) rather than any real effects due to the material or environment—vacuum (Fig. 6a) versus air (Fig. 6b) at 1200 K.

Comparison of the tensile elongation of the as-received and exposed alloy clearly indicates that prior exposure affects ductility. At and below 750 K, the tensile elongation is severely reduced, where the degree of degradation increases as the test temperature is decreased. For example, the as-received alloy 188 possesses about 30% elongation at 750 K in contrast to ~15% after 4900 hr (Fig. 6a) or 10,000 hr (Fig. 6b) of exposure. At 77 K, the as-received material extends more than 30% as opposed to the ~5% elongation for exposed samples. Tensile testing at or above 900 K indicates that prior exposure at 1093 K does not greatly reduce the ductility; in fact, some tendency toward increased elongation exists (1050 and 1200 K testing, Fig. 6b). Neglecting the 1200 K data after 4900 hr of exposure (Fig. 6a), no consistent, significant differences in behavior exist among the tensile elongation results from samples exposed to either molten LiF-22CaF$_2$, salt vapor, vacuum, or air.

3.2.4 *Structure of Tensile Tested Alloy 188*

Typical examples of the microstructure of as-received and exposed alloys after tensile testing are presented in Fig. 7. In general, all exposure conditions (salt, vacuum, or air for 4900 and 10,000 hr at 1093 K) yielded similar microstructures at each of the six tensile test temperatures. Such a result was expected, because the residual tensile properties of the exposed alloy 188 specimens were, for all practical purposes, identical. The only major change in structure involved differences among

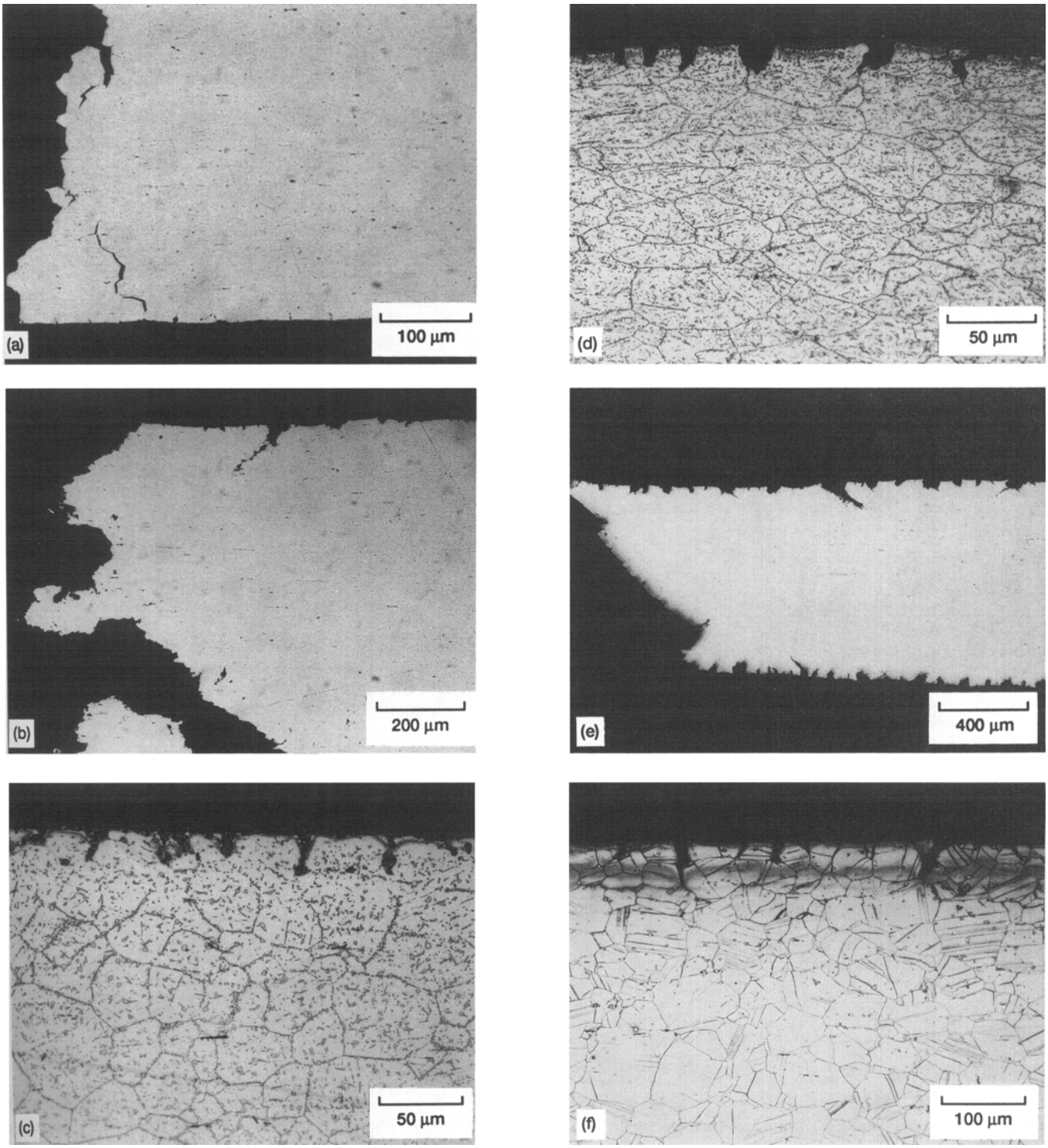

Part	Test temperature, K	Prior exposure conditions	0.2% yield strength, MPa	UTS, MPa	Elongation, %
(a).....	77	4900 hr, air	769	1186	2.7
(b).....	1050	10,000 hr, vapor	288	457	26
(c).....	77	10,000 hr, air	480	1012	4.2
(d).....	1050	10,000 hr, air	281	489	26
(e).....	1050	10,000 hr, liquid	301	446	26
(f).....	1050	As received	305	488	16

Fig. 7 Representative photomicrographs of the microstructure of tensile tested Haynes® Alloy in the vicinity of fracture surface. **(a)**, **(b)**, and **(e)** are unetched; **(c)**, **(d)**, and **(f)** are etched.

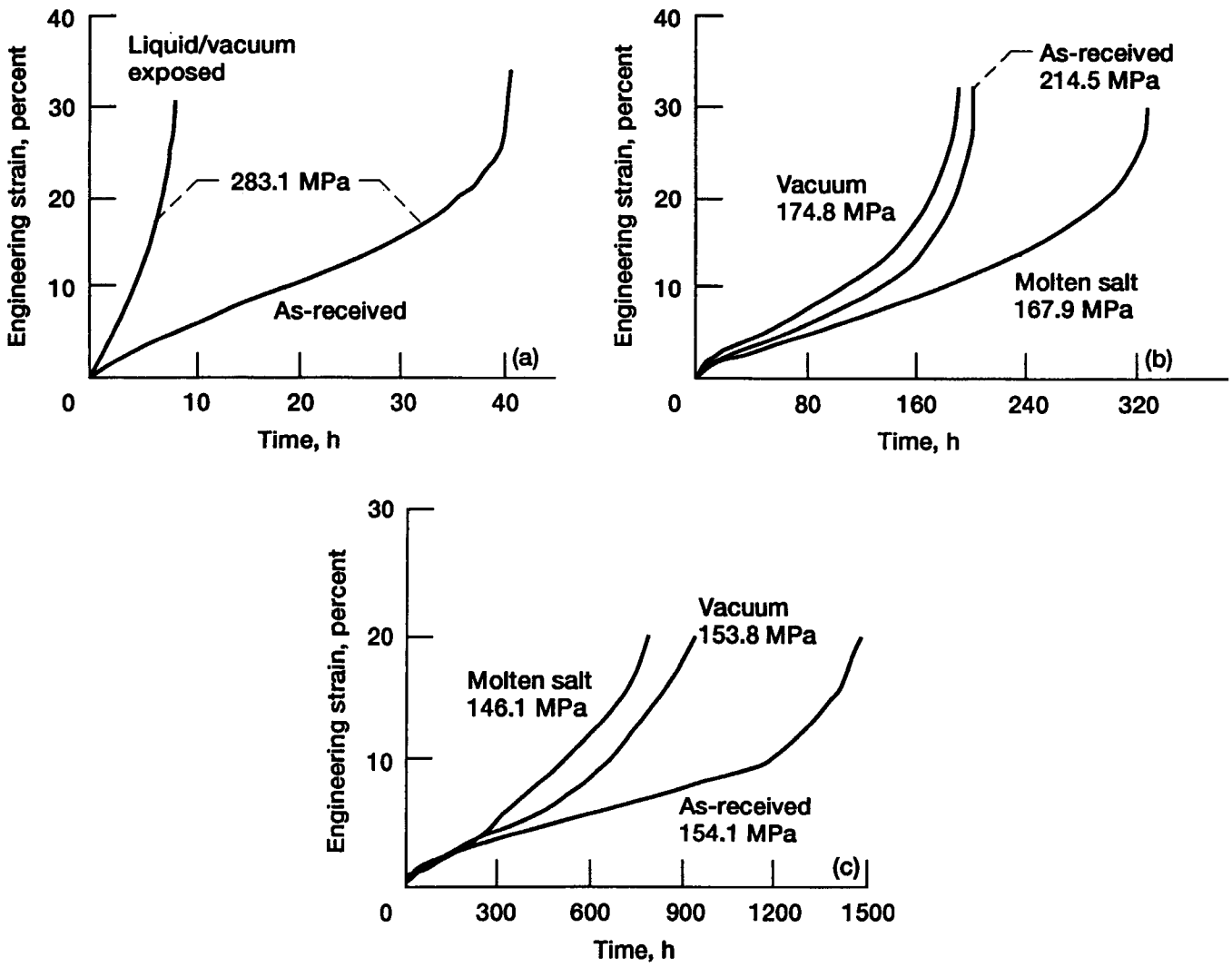

Fig. 8 Representative engineering creep curves for as-received, molten salt-, and vacuum-exposed Haynes® Alloy tested in vacuum at 1050 K. Prior exposures undertaken at 1093 K for 10,000 hr. **(a)** Short, **(b)** intermediate, and **(c)** long lifetimes.

the low and intermediate temperature (≤900 K) tensile fracture of as-received and exposed samples. As illustrated in Fig. 7(a), low-temperature tensile failure in all exposed alloy 188 occurred intergranularly, and such a tendency takes place up to at least 750 K. At and above 1050 K, previously exposed alloy 188 is quite plastic and fractures via transgranular shear and tearing (Fig. 7b). Testing of exposed alloy at 900 K, in most cases, yielded signs of both inter- and intragranular mechanisms at the failure sites. On the other hand, as-received alloy 188 exhibited ductile, intragranular fracture at all test temperatures.

The presence of the pits in either air-exposed (Fig. 2f) or molten salt-exposed (Fig. 2c) alloy 188 did not initiate catastrophic grain boundary failure during either low- (Fig. 7c) or high- (Fig. 7d) temperature tensile testing. Although deep surface-connected cracks were formed in samples with pre-existing flaws (Fig. 7e), the same type of grain boundary cracking was found after 1050 and 1200 K testing of unblemished (as-received, LiF-22CaF_2 vapor, or vacuum exposures) materials (Fig. 7f).

3.3 *1050 K Creep-Rupture Testing*

Typical creep curves for alloy 188 tested in vacuum at 1050 K are illustrated in Fig. 8 as a function of the engineering stress and prior exposure condition. These data are typical of all tested materials, where the normal three stages of creep are present during short- (Fig. 8a), intermediate- (Fig. 8b), and long-term (Fig. 8c) testing. In the course of this study, as-received alloy 188 was creep tested at both contractors, and the results of their testing in terms of time-to-failure, t_r, and the engineering steady-state creep rate, $\dot{e}$, are shown in Fig. 9. To widen the range of the time-to-failure data, Fig. 9(a) includes the values for the average ultimate tensile strength at 1050 K as an estimate of the stress required to produce rupture in 0.1 hr.

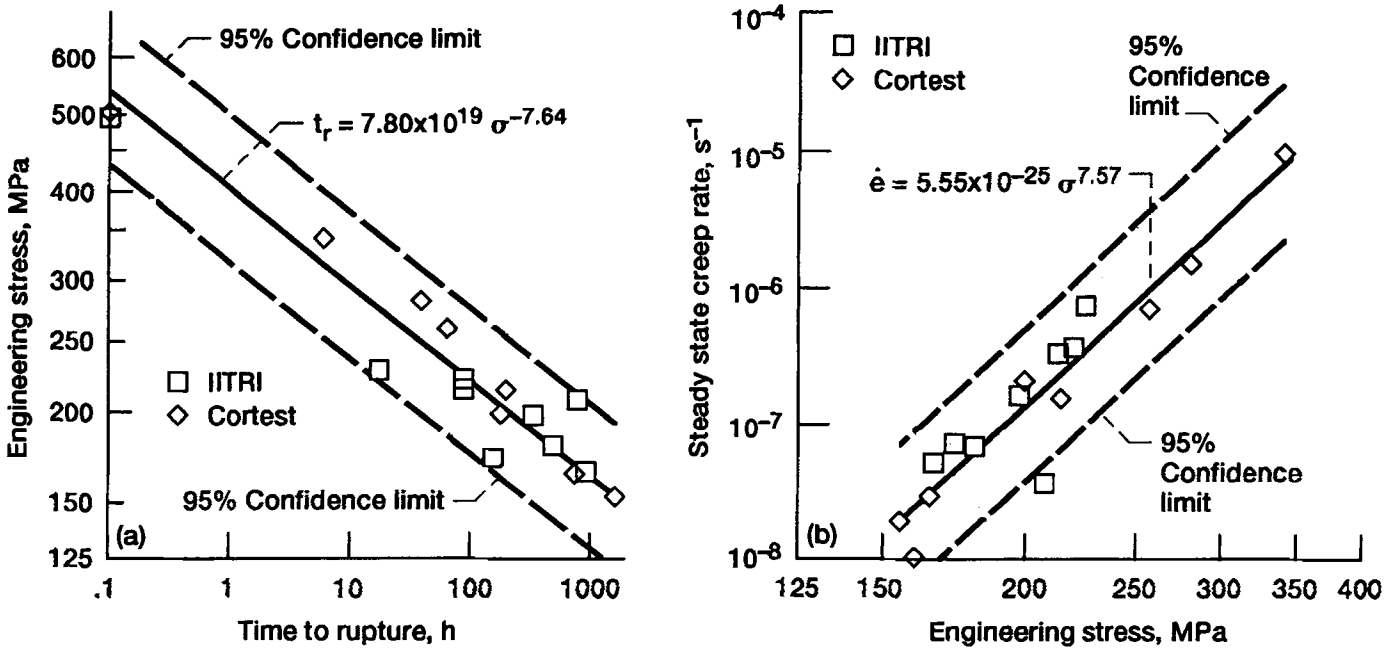

Fig. 9 Time-to-failure (**a**) and steady-state creep rate (**b**) as a function of engineering stress for as-received Haynes® Alloy creep-rupture tested in vacuum at 1050 K.

Table 6 Power Law and Descriptive Statistical Parameters For Haynes® Alloy Creep-Rupture Tested in Vacuum after Exposure to Either Molten LiF-22CaF$_2$ or Vacuum for Various Periods at 1093 K

Testing condition	Constant A, hr	Stress exponent p	Coefficient of determination R_d^2	Standard deviation δ_p
		Time to rupture		
As received	7.80×10^{19}	−7.64	0.922	0.57
Exposed 10^4 hr in molten salt/vacuum	2.82×10^{20}	−8.03	0.976	0.32
Exposed 2500, 4900, or 10^4 hr in molten salt	3.29×10^{19}	−7.67	0.965	0.31
Exposed 2500, 4900, or 10^4 hr in vacuum	4.22×10^{20}	−8.01	0.954	0.37
	B, s^{-1}	n	R_d^2	δ_n
		Steady-state creep rate		
As received	5.55×10^{-25}	7.57	0.891	0.70
Exposed 10^4 hr in molten salt/vacuum	7.14×10^{-25}	7.73	0.972	0.35
Exposed 2500, 4900, or 10^4 hr in molten salt/vacuum (**a**)	1.77×10^{-25}	7.95	0.878	0.47

(**a**) Fit excludes the three 2500-hr vacuum-exposed test results that lie nearest to the stronger 95% confidence limit in Fig. 11(b). Inclusion of these points only slightly changes B and n (9.19×10^{-26} and 8.06, respectively), but reduces R_d^2 to 0.80 and increases δ_n to 0.62.

Both the time-to-failure and creep-rate data followed the usual pattern, where rupture life increased (Fig. 9a) and the creep rate decreased (Fig. 9b) with decreasing stress. Visually, there appeared to be little difference in behavior ascribable to the test vendor, and this was found to be the case by statistical testing with linear regression techniques in combination with a dummy variable and the following power law equations:

$$t_r = A\sigma^p \quad [1]$$

$$\dot{e} = B\sigma^n \quad [2]$$

where A and B are constants, and p and n are stress exponents. Hence, all data were joined and fitted to Eq 1 and 2, and the results of this analysis, as well as the 95% confidence limits, are shown in Fig. 9. The power law parameters and descriptive statistical terms (coefficient of determination, R_d^2, and standard deviations for p and n, δ_p and δ_n) resulting from the fits are given in Table 6.

Examination of the data in Fig. 8 as a whole seems to indicate that the creep strength of 10,000-hr exposed alloy 188 is slightly less than that of the as-received alloy; however, no clear differences in behavior between the molten LiF-22CaF$_2$ or vacuum exposures are visible. This trend is reinforced by the time-to-failure and the engineering steady-state creep-rate data for exposed alloy 188 in Fig. 10. Both the t_r and $\dot{e}$ values are biased toward the weaker 95% confidence limit for as-received alloy 188. Visually, there appears to be little difference in prop-

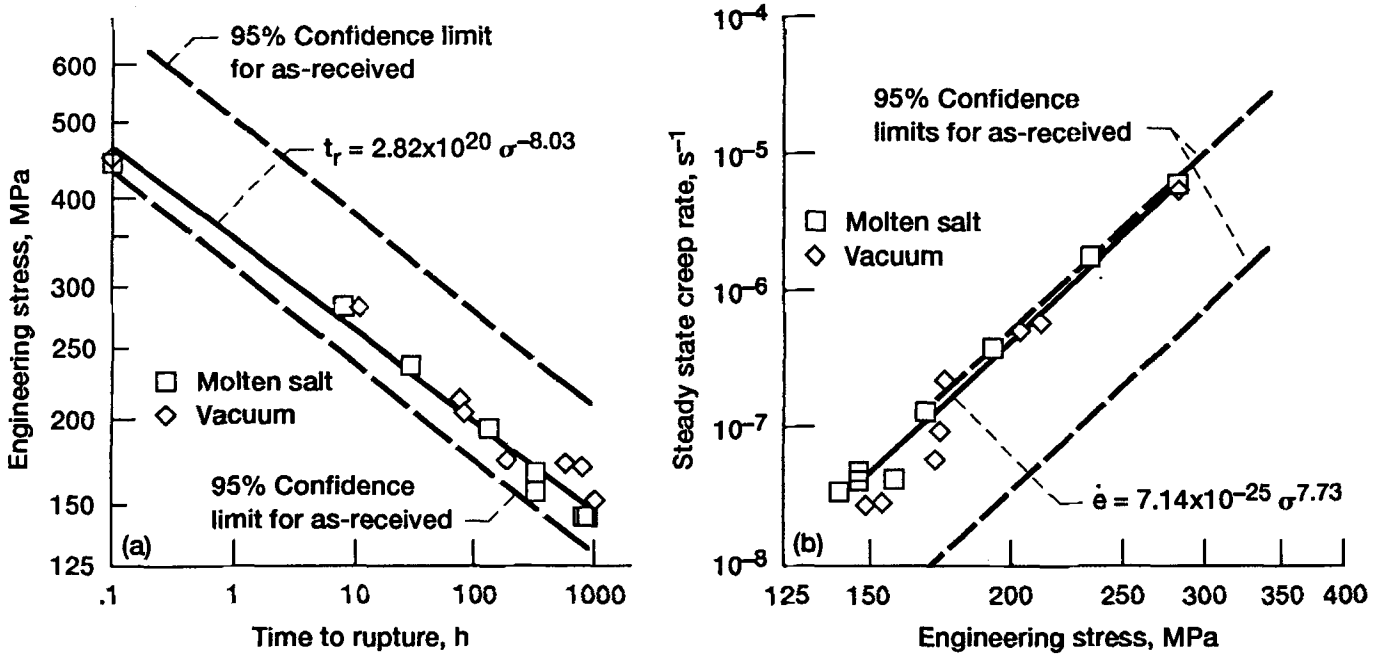

Fig. 10 1050 K vacuum creep-rupture properties for Haynes® Alloy as a function of engineering stress. Specimens subjected to either molten LiF-22CaF_2 or vacuum exposure for 10,000 hr prior to creep-rupture testing. (**a**) Time-to-failure and (**b**) steady-state creep rate.

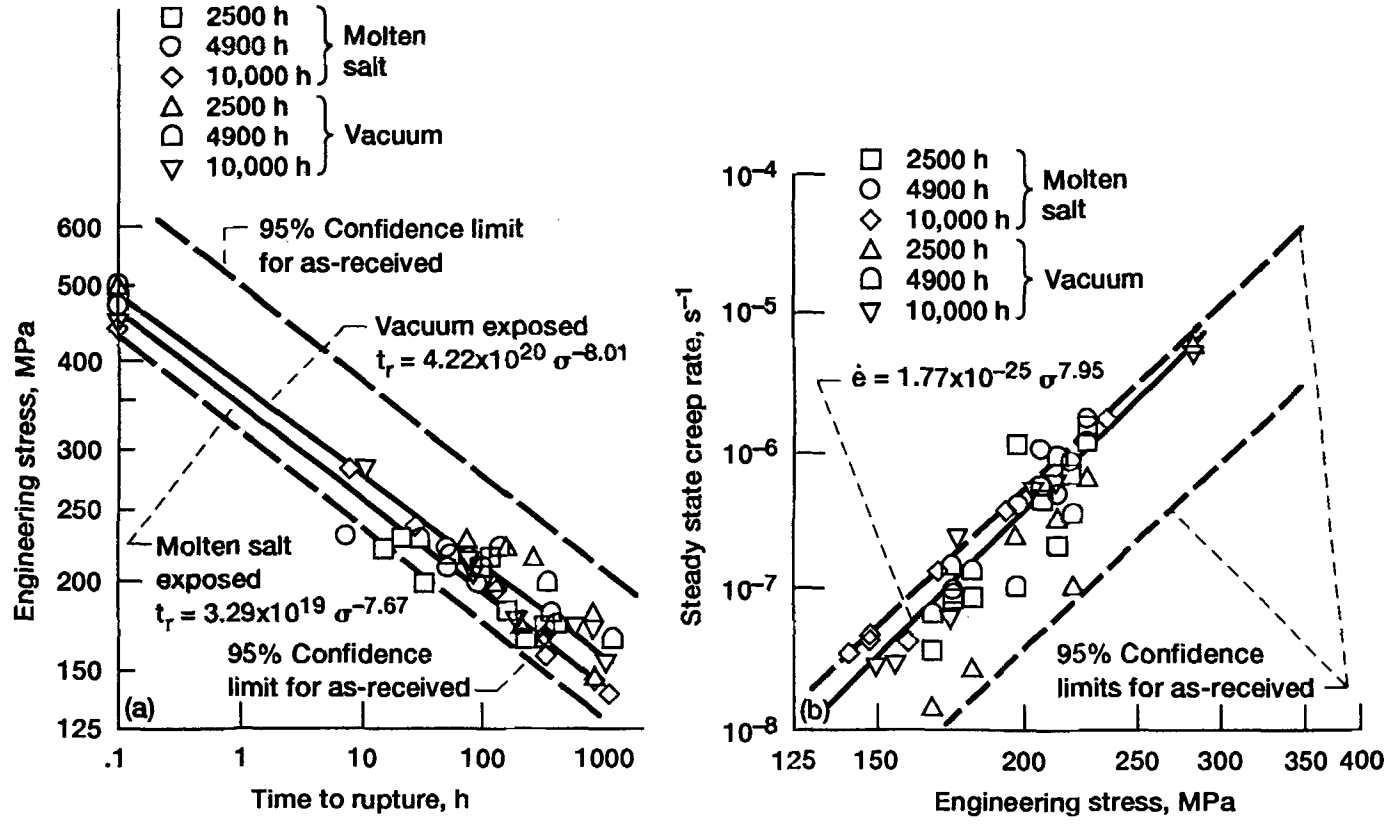

Fig. 11 1050 K vacuum creep-rupture properties for Haynes® Alloy as a function of engineering stress. Specimens subjected to either molten LiF-22CaF_2 or vacuum exposure for 2500, 4900, or 10,000 hr prior to creep-rupture testing. (**a**) Time-to-failure and (**b**) steady-state creep rate.

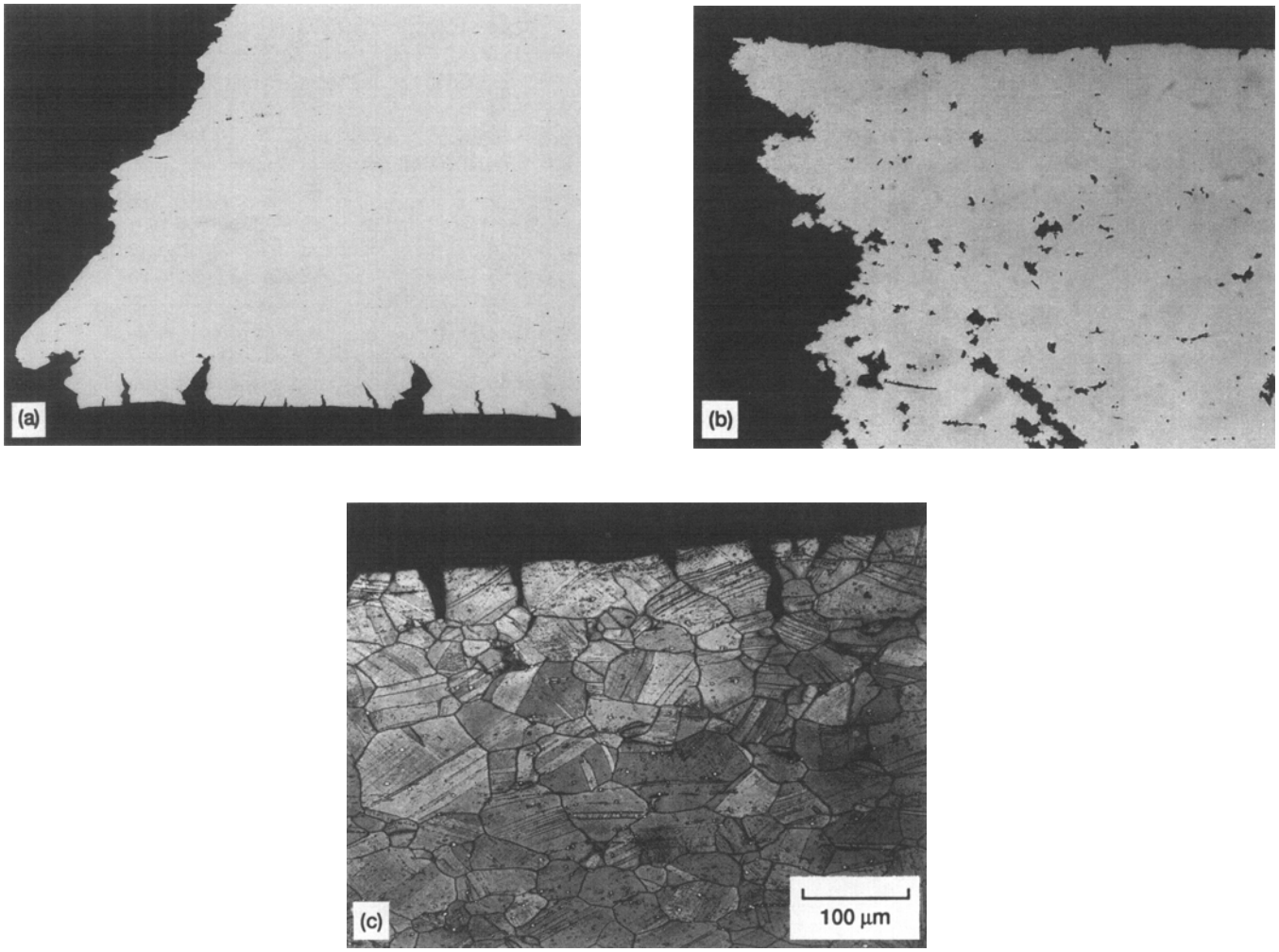

Part	Prior exposure conditions	Stress, MPa	Life, hr	Elongation, %
(a)	As received	209.6	772	21
(b)	10,000 hr, vacuum	171.5	802	30
(c)	As received	267.6	863	34

Fig. 12 Representative photomicrographs of the microstructure of 1050 K vacuum creep-rupture tested Haynes® Alloy. **(a)** and **(b)** Unetched; **(c)** etched.

erties between the molten LiF-22CaF_2 or vacuum-exposed alloy. This latter contention was confirmed by linear regression techniques using a dummy variable and Eq 1 and 2; hence, the data were joined and fitted to the appropriate power laws, and the resultant descriptions for t_r and $\dot{e}$ are given in Fig. 10 and Table 6.

Alloy 188 samples after 2500* and 4900 hr of exposure to molten salt or vacuum have also been vacuum creep-rupture tested at 1050 K, and the time-to-failure and the engineering steady-state creep-rate values are given in Fig. 11 along with the 10,000-hr results. Statistical analysis of t_r data (Fig. 11a) revealed that the vacuum-exposed alloy was slightly stronger than the molten LiF-22CaF_2-exposed alloy 188 alloy. This was primarily due to the higher strength of the 2500-hr samples in comparison to the observed strength after either 4900 or 10,000 hr of vacuum exposure. Although there was a difference in rupture life, such a tendency could not be substantiated in the steady creep-rate values (Fig. 11b). Based on the data in Fig. 11, any prior 1093 K exposure tends to weaken alloy 188 in comparison to the as-received properties, but the strength of essentially all exposed specimens still lies within 95% confidence limits for the as-received alloy.

Selected creep-rupture tested samples were metallographically prepared and examined, and typical microstructures are presented in Fig. 12. In most cases, the final fracture was a result of surface-connected intergranular cracks and ductile fail-

*2500-hr exposed specimens possessed a smaller gage section (6.35 by 25.4 mm).[2]

ure mechanisms generally in combination with shear (Fig. 12a) due to overload conditions during the last few moments of life. The only distinct difference in the post-creep-rupture-tested structure ascribable to prior history was the presence of small cracks and pores beneath the primary fracture in the exposed samples (Fig. 12b); such features were generally not visible in the as-received alloy (Fig. 12a). All samples possessed surface-connected grain boundary cracks (Fig. 12c), and all exposed specimens contained heavy precipitation of inter- and intragranular carbides. In general, the 1050 K creep-rupture samples have the same appearance as the 1050 K tensile specimens.

4. Discussion

Studies[2] on the effects of 400 and 2500 hr of exposure at 1093 K to molten LiF-22CaF_2, its vapor, and vacuum on the tensile properties and structure of alloy 188 have been expanded to include:

- Longer exposure times of 4900 and 10,000 hr
- 1050 K vacuum creep-rupture testing of molten salt and vacuum-exposed samples
- Exposures in air at 1093 K

None of these additional evaluations have uncovered evidence that is contrary to the original finding[2] that this alloy is suitable for containment of the eutectic LiF-CaF_2 thermal energy storage media.

To be sure, long-term exposure of alloy 188 at 1093 K did produce some obvious differences in comparison to the as-received material. In particular, inter- and intragranular precipitation of carbides occurred during all exposures (Fig. 2b). Although some minor attack was found on the molten salt-exposed surfaces (Fig. 2c), the salt vapor- or vacuum-exposed surfaces were not corroded (Fig. 2d). The vacuum-exposed samples lost weight through evaporation of chromium and manganese (Table 2), whereas long-term annealing in air produced a weight gain (Table 3) from the formation of an oxide scale. Furthermore, the air-exposed alloy developed pits (Fig. 2f) that grew along grain boundaries into the base metal.

The most significant finding during subsequent tensile testing of 1093 K exposed specimens is the substantially decreased ductility at the lower test temperatures (77, 298 and 750 K, Fig. 5) in comparison to the plasticity of the as-received alloy. Such low-temperature embrittlement of alloy 188 after elevated temperature exposure is a well-known phenomenon[2,6] and results from carbide precipitation, which leads to a change in fracture mechanism from intragranular in the as-received condition to intergranular after exposure. This change in fracture mechanism was independent of the specific environment, with salt-, vacuum-, and air-exposed specimens undergoing the same degradation (Fig. 5). Consequently, the decrease in lower temperature tensile ductility is due to a thermal effect rather than a corrosive attack.

Creep-rupture testing of alloy 188 at 1050 K following long-term (2500 to 10,000 hr) molten salt or vacuum exposures revealed that prior 1093 K treatments slightly weaken this alloy (Fig. 10 and 11) relative to the as-received properties. However, both the time-to-failure and steady-state creep-rate data for the exposed samples fell within the 95% confidence limits for the as-received properties. Therefore, any degradation in creep-rupture behavior as a result of prior exposure is minor at worst and, based on statistical testing of the data, is essentially independent of the particular environment. These results, once again, indicate that any measurable changes in the behavior of alloy 188 are ascribable to thermal effects rather than corrosion.

5. Conclusion

Based on a study of the structure, tensile properties, and creep-rupture characteristics of alloy 188 after 1093 K exposures lasting as long as 10,000 hr in vacuum, air, molten LiF-22CaF_2, and its vapor, it was found that none of these diverse environments produced any significant changes beyond those ascribable to simple thermal treatments. Therefore, it is concluded that alloy 188 is a suitable containment alloy for LiF-CaF_2-based thermal energy storage systems.

References

1. T.L. Labus, R.R. Secunde, and R.G. Lovely, "Solar Dynamic Power Module Design," Paper No. 899277, *Proceedings of the 24th Intersociety Energy Conversion Engineering Conference*, Institute of Electrical and Electronics Engineers, Vol. 1, IEEE, New York, 299-307 (1989).
2. J.D. Whittenberger, *J. Mater. Eng.*, *12*, 211-226 (1990).
3. J.D. Cotton and L.M. Sedgwick, "Compatibility of Selected Superalloys with Molten LiF-CaF_2 Salt," Paper No. 899235, *IECEC'89*, Vol. 2, IEEE, New York, 917-921 (1989).
4. H.J. Strumpf, R.P. Rubley, and M.G. Coombs, "Material Compatibility and Simulation Testing for the Brayton Engine Solar Receiver for the NASA Space Station Freedom Solar Dynamic Option," Paper No. 899076, *IECEC'89*, Vol. 2, IEEE, New York, 895-903 (1989).
5. H.J. Strumpf, R.P. Rubley, and M.G. Coombs, "Solar Receiver Thermal Energy Storage Canister Compatibility Test," AiResearch Division, Allied-Signal Aerospace Company, Los Angeles, CA, Report No. 90-64179 (1990).
6. Haynes International Data Sheet for Haynes® Alloy 188, Haynes International, Kokomo, IN.
7. J.D. Whittenberger, *J. Mater. Energy Systems*, *8*, 385-390 (1987).
8. J.D. Whittenberger, *J. Mater. Eng.*, *10*, 247-258 (1988).